Since January 2020 Elsevier has created a COVID-19 resource centre with free information in English and Mandarin on the novel coronavirus COVID-19. The COVID-19 resource centre is hosted on Elsevier Connect, the company's public news and information website.

Building and Environment 196 (2021) 107788

Contents lists available at ScienceDirect

Building and Environment

journal homepage: http://www.elsevier.com/locate/buildenv

Probable airborne transmission of SARS-CoV-2 in a poorly ventilated restaurant

Yuguo Li [a,h,1], Hua Qian [b,1], Jian Hang [c,1], Xuguang Chen [d], Pan Cheng [a], Hong Ling [c], Shengqi Wang [b], Peng Liang [e], Jiansen Li [d], Shenglan Xiao [a,i], Jianjian Wei [f], Li Liu [g], Benjamin J. Cowling [h], Min Kang [d,*,1]

[a] Department of Mechanical Engineering, The University of Hong Kong, Hong Kong, China
[b] School of Energy and Environment, Southeast University, Nanjing, China
[c] School of Atmospheric Sciences, Sun Yat-sen University and Key Laboratory of Tropical Atmosphere-Ocean System, Ministry of Education, Zhuhai, China
[d] Guangdong Provincial Center for Disease Control and Prevention, Guangzhou, China
[e] Guangdong Field Epidemiology Training Program, Ganzi Tibetan Autonomous Prefecture Center for Disease Control and Prevention, Sichuan, China
[f] Institute of Refrigeration and Cryogenics and Key Laboratory of Refrigeration and Cryogenic Technology of Zhejiang Province, Zhejiang University, Hangzhou, China
[g] School of Architecture, Tsinghua University, Beijing, China
[h] School of Public Health, The University of Hong Kong, Hong Kong, China
[i] School of Public Health, Sun Yat-sen University, Shenzhen, China

ARTICLE INFO

Keywords:
COVID-19
SARS-CoV-2
Airborne transmission
Aerosol transmission
Building ventilation

ABSTRACT

Although airborne transmission of severe acute respiratory syndrome coronavirus 2 (SARS-CoV-2) has been recognized, the condition of ventilation for its occurrence is still being debated. We analyzed a coronavirus disease 2019 (COVID-19) outbreak involving three families in a restaurant in Guangzhou, China, assessed the possibility of airborne transmission, and characterized the associated environmental conditions. We collected epidemiological data, obtained a full video recording and seating records from the restaurant, and measured the dispersion of a warm tracer gas as a surrogate for exhaled droplets from the index case. Computer simulations were performed to simulate the spread of fine exhaled droplets. We compared the in-room location of subsequently infected cases and spread of the simulated virus-laden aerosol tracer. The ventilation rate was measured using the tracer gas concentration decay method. This outbreak involved ten infected persons in three families (A, B, C). All ten persons ate lunch at three neighboring tables at the same restaurant on January 24, 2020. None of the restaurant staff or the 68 patrons at the other 15 tables became infected. During this occasion, the measured ventilation rate was 0.9 L/s per person. No close contact or fomite contact was identified, aside from back-to-back sitting in some cases. Analysis of the airflow dynamics indicates that the infection distribution is consistent with a spread pattern representative of long-range transmission of exhaled virus-laden aerosols. Airborne transmission of the SARS-CoV-2 virus is possible in crowded space with a ventilation rate of 1 L/s per person.

1. Introduction

Following a debate of airborne transmission of SARS-CoV-2 [1], the virus that causes COVID-19, in the continuing COVID-19 pandemic, leading health authorities have recognized the importance of airborne transmission in special settings since October 2020 [2,3]. The well-known Wells-Riley equation [4] suggests the importance of sufficient building ventilation in diluting the infectious aerosols. However, the effective minimum ventilation rate for avoiding airborne transmission remains unknown. Existing ventilation standards such as ASHRAE 62.1-2019 [5] do not consider infection control as their objectives. The Wells-Riley equation or its variants may be used to determine the minimum ventilation rate if the quanta generation rate is known, however, significant uncertainty exists in the existing available

* Corresponding author. Guangdong Provincial Center for Disease Control and Prevention, No.160 Qunxian Road, Panyu District, Guangzhou, Guangdong, 511430, PR China.,
E-mail addresses: liyg@hku.hk (Y. Li), kangmin@cdcp.org.cn (M. Kang).
[1] These authors contributed equally.

https://doi.org/10.1016/j.buildenv.2021.107788
Received 1 February 2021; Received in revised form 5 March 2021; Accepted 6 March 2021
Available online 13 March 2021

quanta generation data for COVID-19 [6–8]. Measurement of ventilation rates in the infection venue of an outbreak has been challenging due to difficulties in identification of an airborne outbreak, and difficulties in immediate access to infection venue and data availability of infectors and susceptible in infection venue at the time of infection.

Here we report a detailed epidemiological and environmental study of a restaurant outbreak in Guangzhou, China. The COVID-19 outbreak was identified in early 2020 and linked to three seemingly non-associated clusters of unrelated families (A, B, C) [9]. Families B (n = 4) and C (n = 7) comprised local Guangzhou residents with no history of travel to or encounters with inhabitants from Hubei, but nevertheless three members of family B and two members of family C were confirmed to be infected with SARS-CoV-2 on February 4 or 6, at which time only 322 cases of infection (98 local cases and 224 imported cases) had been confirmed in the city of nearly 13 million residents.

Local health officials learned that families B and C had eaten lunch at the same restaurant on Chinese New Year's Eve (January 24, 2020), as had family A (n = 10) from Wuchang, Wuhan (the epicenter of the Chinese epidemic), who had arrived in Guangdong by train on January 23. One person from family A reported experiencing the onset of COVID-19 symptoms on January 24, and video records from the restaurant show that families A, B, and C were seated at tables along the exterior window, with family A's table in the center. None of the restaurant waiters or remaining 68 patrons distributed at 15 other tables became infected with SARS-CoV-2. Families A, B, and C had not met previously and did not have close contact during the lunch, aside from some patrons sitting back-to-back.

Our field measurement of ventilation was performed in the restaurant with the original table setup on March 19–20. To investigate the possibility of airborne transmission of SARS-CoV-2, we also analyzed the spatial distribution data from this outbreak using computational fluid dynamics (CFD) simulations. We use our results to assess the ventilation conditions of airborne transmission.

2. Methods

2.1. Epidemiologic analysis

We obtained the seating arrangement of the three family members and remaining patrons in Restaurant X as well as the dates of COVID-19 symptom onset, where the symptom onset date is defined as the day when symptoms (e.g., fever or cough) were first noticed by the patient. SARS-CoV-2 infection was confirmed by real-time polymerase chain reaction with reverse transcription (RT-PCR) analysis of throat swabs. Demographic data, travel history, exposure history, and symptoms of the infected individuals were collected [9]. We also obtained the floor plan and design of the air conditioning and ventilation system of the restaurant, and the hourly weather data for January 24 from a weather station near the site. Full closed-circuit television camera records of the restaurant and elevator were reviewed to determine the elevator use by patrons, the fire-door use by both patrons and waiters, the table and seating arrangement during the lunch, and any close contact behavior between Family A and others.

Restaurant X has five floors. The outbreak occurred on the third floor, which has a volume of 431 m^3 (height of 3.14 m, length of 17 m, and average width of 8.1 m) (Fig. 1). Large and small tables have a diameter of 1.8 m and 1.2 m, respectively, and rectangular tables measure 0.9 m × 0.9 m and 1.2 m × 0.9 m. Five fan coil air-conditioning units are installed on the third floor, and there is no outdoor air supply: ventilation is thus achieved using only infiltration and natural ventilation through an occasionally open door driven by buoyancy forces and an exhaust fan installed inside the restroom. Four exhaust fans are

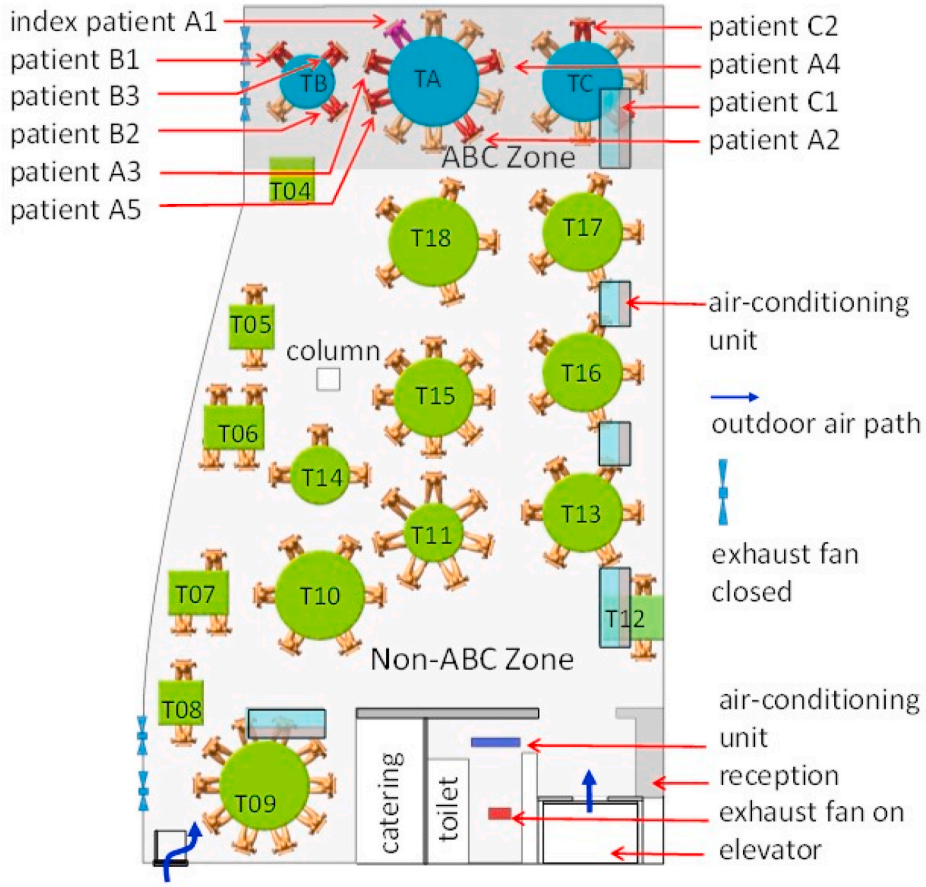

Fig. 1. (Color Online) Distribution of SARS-CoV-2 infection cases at tables in Restaurant X. The probable air-flow zones are shown in dark grey and light grey. Eighty-nine patrons are shown at the 18 tables, with one table being empty (T04). Tables TA, TB, and TC are where families A, B, and C sat, some of whose members became infected. Patient A1 at TA is the suspected index case, who had symptoms shortly after returning to the hotel where Family A was staying. Patients A2–A5, B1–B3, and C1–C2 are the individuals who became infected. Other tables are numbered as T04–T18. Each of the five air-conditioning units (fan coil units) condition a particular zone. Patrons and waiters entered the restaurant floor via the elevator and stairwell, which are connected by the fire door. (For interpretation of the references to color in this figure legend, the reader is referred to the Web version of this article.)

installed on the south glass window but were not used during this lunch. At noon on January 24, the third floor of the restaurant had 18 tables and 89 patrons. We label tables A, B, and C as TA, TB, and TC, respectively, and the remaining tables are labeled as T4–T18 (Fig. 1). According to video analyses, the fire door was used approximately every 2 min.

We studied the infection data with regards to seating location and used a chi-square test to explore the association between a patron's location (i.e., table) and his/her probability of becoming infected. Table A was excluded in this analysis. The other tables were categorized according to two criteria: distance from TA (e.g., immediate vs. remote neighbors) and air-conditioning zone. The ABC zone was that immediately around TA, TB, and TC and serviced by one air conditioning unit, and the non-ABC zone was everywhere else, serviced by the four other air conditioning units.

2.2. Experimental tracer gas measurements and computational fluid-dynamics simulations

Tracer gas measurements and computational fluid dynamics (CFD) simulations were used to predict the spread of fine droplets exhaled by the index case and the detailed airflow pattern in the restaurant. The CFD simulation models were the same as those used in previous studies of two 2003 Severe Acute Respiratory Syndrome coronavirus (SARS-CoV) outbreaks in Hong Kong [10–12].

The tracer measurement was carried out on March 19–20 when the intensity of the direct solar radiation was similar to that on January 24, i.e., weak sunshine, with clouds and rain. We first measured the supply/return/exhaust air flow and temperature at each air-conditioning unit and at the exhaust fan in the restroom. We arranged the tables and chairs to match the arrangement used at the January 24 lunch, as determined by the video analyses. The air conditioning units were turned on and the exhaust fans in the vertical glass window were left off to simulate the airflow conditions at the time of SARS-CoV-2 infection during the lunch on January 24. Volunteers were not recruited because the experiment was performed during the strict intervention (i.e., partial lockdown) phase of the epidemic in Guangzhou. However, nine of our team members volunteered to sit at tables A, B, and C and simple thermal mannequins were placed at the others. The mannequins were warm and hollow, containing a 60-W electrical bulb enclosed by a stainless steel cylinder, which produced warm plumes similar to those produced by the human volunteers. A 60-W electrical bulb was also used to simulate warm food on each table.

The tracer gas measurement consisted of two stages. In the first stage, we released ethane gas through an 8-mm inner diameter pipe at a speed of 1.5 m/s at 32–34 °C, with the pipe outlet placed immediately above the index case's nose. This mode of release mimicked the index case (assumed to be A1) talking and moving their head around. Tracer gas is known to be an effective surrogate for modeling the spread of fine droplets or droplet nuclei [13]. In the first of two experiments, we monitored the gas concentrations at 14 points, namely all of the chairs where the infected members of families B and C had sat (Figure C1). In the second experiment, gas concentrations were only monitored at seven points, owing to the time required for rotational sampling at each point.

In the second stage, the ventilation rate was measured using the tracer concentration decay method, which involved the release of a tracer gas into the restaurant and subsequent mixing with the flow from 10 desk fans. We measured the tracer concentration at three points in the room. The elevator and fire door were opened every 2 min to mimic the traffic that was observed in the recording of the January 24 lunch, with the fire door closing automatically after a period of 3 s. We identified an exhaust flow through the doorway of the restroom and bidirectional air exchange through the opening and closing of the fire door. The non-operating exhaust fans were sealed relatively well, with nearly negligible air flow. After the measurements, we assigned the health status (ill vs. healthy) of each person at non-A tables as the dependent variable and applied a binary logistic regression model to investigate the association between the measured concentrations of tracer gas and infection probability.

We adopted the widely used CFD software package Fluent (Ansys Fluent, USA), which is a three-dimensional, general-purpose CFD software package for modeling fluid flows. We used the basic renormalization-group (RNG) k-ε turbulence model to simulate the effects of turbulence on airflow and dispersion of pollutants. We assumed that the virus-laden water droplets generated from the index case at TA rapidly evaporated (i.e., after a few s in air). We first approximated the exhaled droplet nuclei as a passive scalar, as in the experiments, and the deposition effect was therefore neglected. The prediction was then compared to the measured value. Next, we considered the deposition of droplet nuclei (using a drift-flux model of Ref [14]), filtration of the air conditioning units (with a filtration efficiency of 20% following a preliminary measurement on site), and deactivation of the virus in aerosols [15], and predicted the temporal concentration profiles of the droplet nuclei containing the virus, which was then used to calculate the total exposure at each table. Only a representative droplet nuclei size of 5 μm is modeled, and its surface deposition was ignored as the deposition loss of fine droplet nuclei is significantly small compared to virus deactivation [8]. After CFD modeling, we used the health status (ill vs. healthy) of each person at non-A tables as the dependent variable and applied a binary logistic regression model to investigate the association between the predicted concentration of tracer gas and predicted exposure to droplet nuclei and infection probability.

3. Results

3.1. The outbreak

Detailed epidemiological, clinical, laboratory, and genomic findings for this outbreak and all of the associated patients have been described in detail by Ref. [9]. The first confirmed case (A1) from family A, who was confirmed on January 24, is assumed to be the index case (Fig. 1). Patient A1 first had symptoms of a fever and cough in the late afternoon of January 24 (Fig. 2A, Table A1). The last patient was confirmed on February 6 (Fig. 2B). The three families occupied the restaurant at different times (family A 12:01–13:23; family B 11:37–12:54; and family C 12:03–13:18). According to the video analysis, there was no significant close contact between the three families in the elevator or restroom (Supplementary information B). Contact tracing identified 68 patrons on the third floor at the same time as families A, B, and C, and 102 patrons on other floors. We also identified 57 workers in the restaurant including 8 on the third floor, a taxi driver who had A1 as a customer on the afternoon of January 24, and 11 workers in the hotel where family A stayed. The hotel is within walking distance of the restaurant. All of these close contacts were identified after February 7. Only 11 non-infected members of families A, B, and C were quarantined in a central facility; throat swab samples were taken but yielded negative results for SARS-CoV-2. The 8 restaurant workers on the third floor, 11 hotel workers, and 19 patrons at other third-floor tables were home quarantined for 14 days and their symptoms were continuously monitored. The remaining identified contacts were only followed up by telephone and none reported any symptoms. Thus, only the 10 patrons in the restaurant were infected, comprising the index case and nine others, including the five members of families B and C who are assumed to have been infected at this lunch due to exposure to exhaled droplets from the index case that contained virus particles. Families B and C had no close contact with any known COVID-19 patients and/or visitors from Hubei Province 14 days prior to the onset of their symptoms (Figure D1). Although various scenarios of transmission are possible (e.g., C2 may have become infected while caring for C1) [9], determined that at least one member from both families B and C was exposed to SARS-CoV-2 at the restaurant.

The arrival and departure times of patrons at all tables are listed in

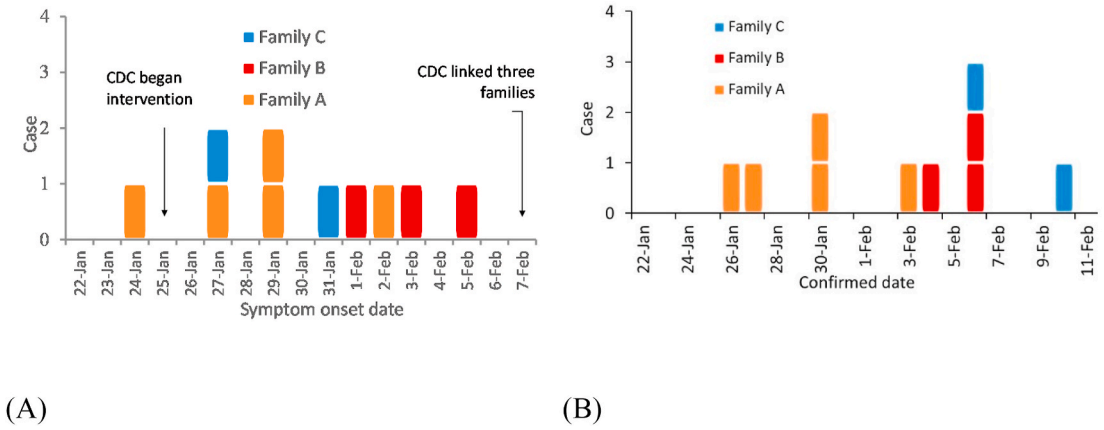

Fig. 2. (Color Online) Dates of (A) symptom onset and (B) confirmation of the 10 patients from the three families. Patients from family A, B, C are represented by yellow, red and blue squares respectively. (For interpretation of the references to color in this figure legend, the reader is referred to the Web version of this article.)

Table 1
Arrival, departure, and overlap time.

Table	Arrival (first patron at table)	Departure	Lunch duration (min)	Starting exposure	Overlap with Table A (min)	Total exposure time (min)	Period of exposure after Table A's departure (min)
TA	12:01	13:23	82	12:01	82	82	0
TB	11:37	12:54	77	12:01	53	53	0
TC	12:03	13:18	75	13:00	75	77	0
T05	11:32	12:53	81	12:01	52	52	0
T06	11:36	13:23	107	12:01	82	82	0
T07	11:29	13:10	101	12:01	69	69	0
T08	12:28	13:37	69	12:28	55	69	14
T09	11:47	13:16	89	12:01	75	75	0
T10	11:07	13:28	141	12:01	82	82	5
T11	11:32	13:11	99	12:01	70	70	0
T12	12:13	13:17	64	12:13	64	64	0
T13	11:53	12:51	58	12:01	50	50	0
T14	11:23	13:02	99	12:01	61	61	0
T15	11:55	13:30	95	12:01	82	89	7
T16	11:24	12:49	85	12:01	48	48	0
T17	13:00	14:19	79	13:00	23	79	56
T18	11:34	13:18	104	12:01	77	77	0

Table 1. Upon arriving at the restaurant, families A, B, and C took the elevator to the third floor and did not remain in the reception area, as they had previously booked tables. Family A used the elevator in two groups. One patron from T18 shared the lift with the first group. The second comprised the remaining two members of family A. Families B and C and patient C1 used the elevator separately.

Shortly after being seated, patient A4 and two unaffected females of family A left their table to use the restroom. During the meal, patient A4 left the table two additional times to go to the catering room to retrieve new chopsticks or a spoon. An unaffected male member of family C used the restroom shortly after sitting down and overlapped there for 1 min with three members of family A. Some members of the three families used the restroom immediately prior to leaving the restaurant. No sharing of items (e.g., a kettle) was observed between the three tables and no conversations occurred between the three families. During the meal, the patrons at TA were active, with instances of members standing up and talking to the left and right, whereas patrons at TB and TC were comparatively inactive.

3.2. Spatial distribution analysis of infection cases

The tables and patrons were first categorized by distance from TA, as immediate neighbors (TB, TC, and T18) or remote neighbors (tables T4–17). The 10 patients who were shortly thereafter confirmed as having COVID-19 sat at one of the three tables by the window. Three of the four members of family B were infected, and two of the seven members of family C were infected. Five members of family A were also infected, including the index case. The two patrons at TC who sat the closest to TA were not infected, nor were any patrons at the remote neighboring tables, but the patrons at neighboring tables had a higher infection probability than patrons at remote tables ($\chi^2 = 16.08$, $P < 0.001$, chi-squared test with continuity correction, Table 2). The infection risk was also higher for patrons at zone-ABC tables than those at non-ABC zone tables ($\chi^2 = 25.78$, $P < 0.001$). None of the patrons seated in the non-ABC zone were infected.

3.3. Ventilation and dispersion of exhaled droplet nuclei

The results of the two tracer gas decay experiments show that the air exchange rate was only 0.77 air changes per hour (ACH) at 16:00–17:00 and 0.56 ACH at 18:00–19:30 (Figure C2). For a volume of 431 m^3 and 89 patrons, this is equivalent to an outdoor air supply of 1.04 and 0.75 L/s per patron, respectively. The average measured ventilation rate is 0.9 L/s per person.

The predicted contaminated cloud envelope in the ABC zone is shown in Fig. 3. The exhaled air stream from the index case rises in the zone with families A, B, and C, following the interaction of thermal plumes and the air jet of the air conditioning (Fig. 4). The high-momentum air-conditioning jet carries the contaminated air at ceiling height. Upon reaching the opposite glass window, the jet bends downward and returns at a lower height. At each table, the rising thermal plumes from the warm food and people carry the contaminated air

Table 2
Number of cases and susceptible patrons at non-A tables in different zones of Restaurant X. There were a total of 79 patrons at the other 17 tables.

Category of zones	Zones	Number of patrons	Number of infected cases	Attack rate (%)	*RD** (95% CI)	χ^2	*P*
Table A neighbors	Immediate neighboring tables	16	5	31.25	31.25 (8.54, 53.96)	16.08#	<0.001#
	Remote neighboring tables	63	0	0			
Air conditioning	ABC zone	11	5	45.45	45.45 (16.03,74.88)	25.78#	<0.001#
	Non-ABC zone	68	0	0			

**RD*: Rate difference.
Chi-squared test with continuity correction.

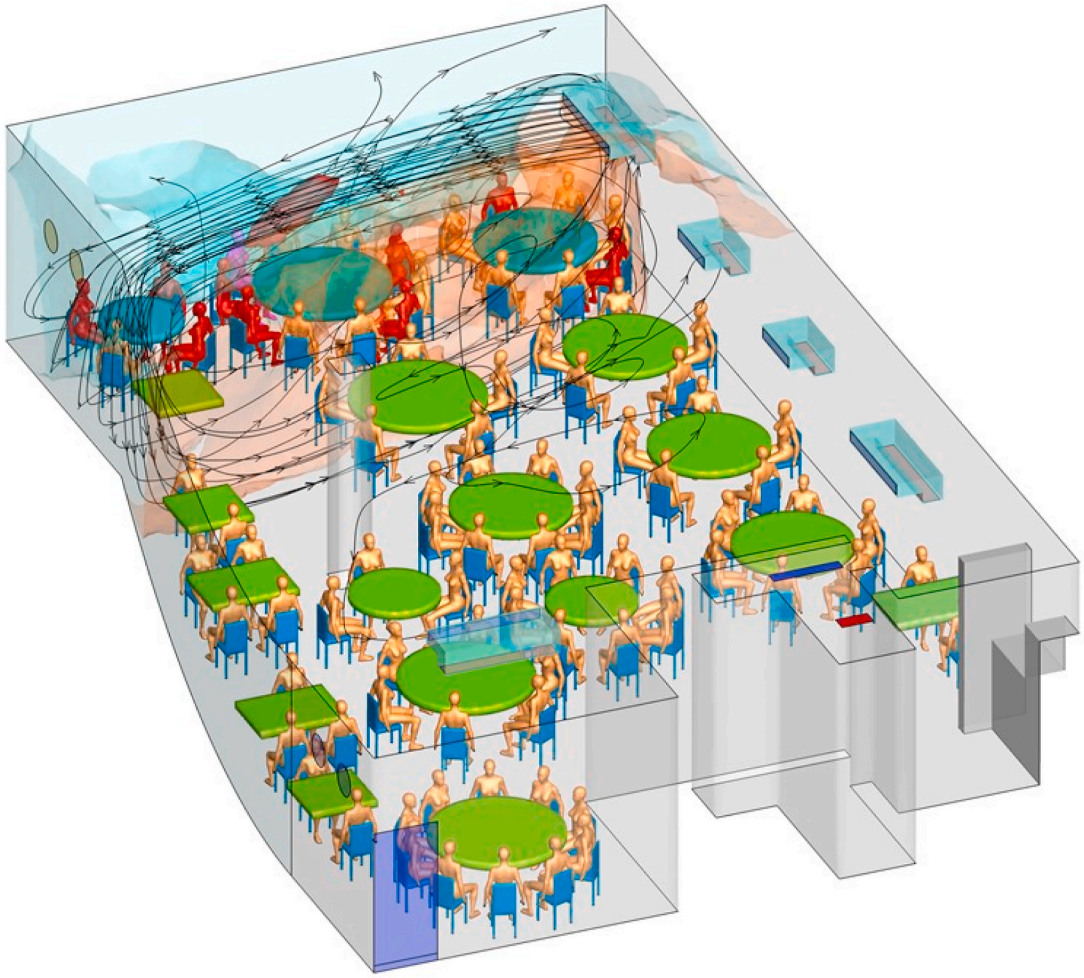

Fig. 3. (Color Online) Simulated dispersion of fine droplets exhaled from index case A1 (purple), which are initially confined within the cloud envelope (ABC bubble) due to the zoned air-conditioning arrangement. The fine droplets disperse into the other zone via air exchange and are eventually removed via the restroom exhaust fan. The streamlines originated from the ABC air conditioning unit are plotted to show the formation of the ABC bubble. The ABC zone clearly has a higher concentration of fine droplets than the non-ABC zone. Other infected patients are shown in red and non-infected patrons in gold. (For interpretation of the references to color in this figure legend, the reader is referred to the Web version of this article.)

upward, and the remaining air returns to the air-conditioning unit and forms a recirculation zone or bubble, referred to as the ABC zone. Similarly, other air-conditioning units also produce cloud envelopes, although these are not as distinct as that in the ABC zone, due to mixing by the air-conditioning jet of the air-conditioning unit above T09. Air exchange occurs between all of the zones because there are no physical barriers between them. Spread of exhaled droplet nuclei in the restaurant is also shown in an animation shown in Appendix B as predicted by computational fluid dynamics.

The formation of a relatively isolated contamination cloud in the ABC zone is supported by both the measured ethane concentration data and predicted droplet nuclei concentration data. The average measured ethane concentrations over a period of 66.67 min (Table 3) at TA, TB, and TC are the highest, being 1.00, 0.92, and 0.96 (normalized by the concentration at TA), respectively, whereas the concentrations are 0.86 and 0.73 at T17 and T18, respectively, and 0.55–0.70 at the other remote tables. As expected, some mixing clearly occurred between the different air-conditioning zones (Fig. 4), although a stable higher concentration was maintained in the ABC zone. The predicted normalized ethane concentrations agree well with the measured values (Fig. 5).

We use the predicted concentrations of infectious virus-containing droplet nuclei (5 μm) in the restaurant (Fig. 6) to calculate the exposure using the exposure duration data in Table 1. When the deposition, filtration, and virus deactivation are considered, the predicted normalized time-averaged concentrations of the infectious virus-containing droplet nuclei (5 μm) during the entire period of TA's presence reveal

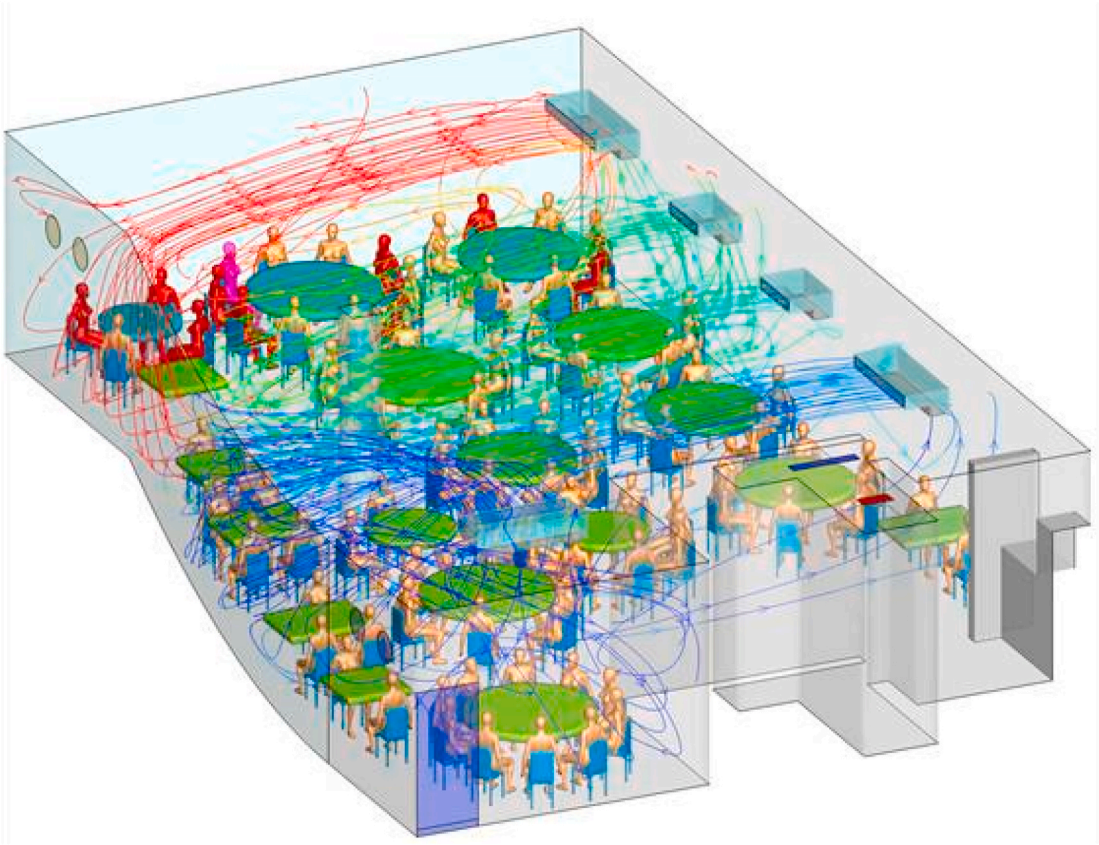

(A)

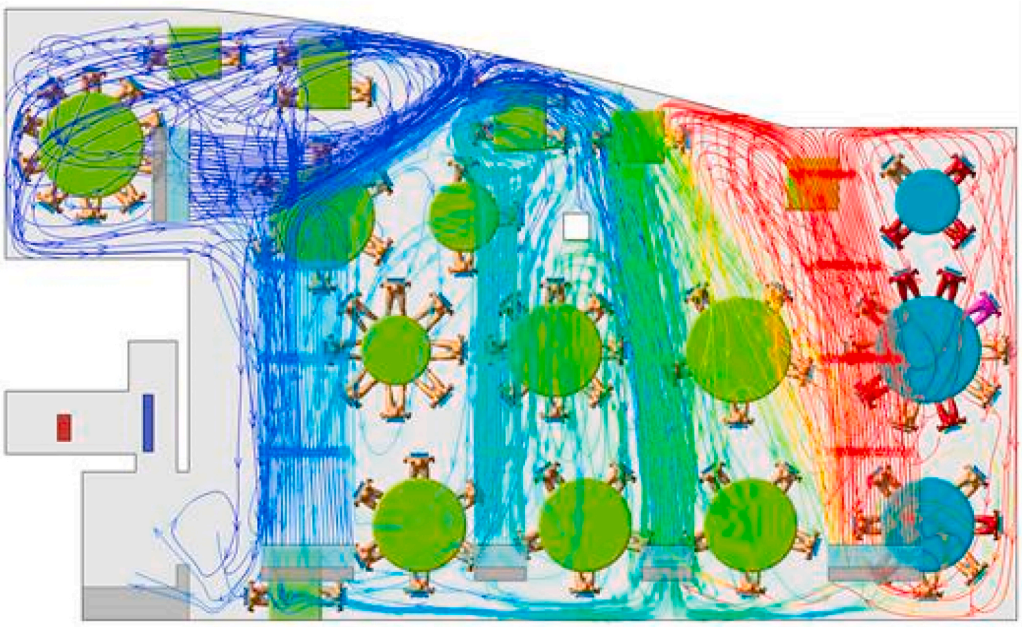

(B)

Fig. 4. (Color Online) Simulated air streamlines originating from the air conditioning units in the restaurant using computational fluid dynamics. The index case A1 is shown in purple, other infected patients in red, and non-infected in gold. The streamlines are colored by the concentration of predicted infectious droplet nuclei, with red the highest and blue the lowest. (A) 3D view and (B) top view. (For interpretation of the references to color in this figure legend, the reader is referred to the Web version of this article.)

Table 3
Number of cases and susceptible patrons (n = 89) at the 18 different tables of Restaurant X during lunch on January 24, 2020.

Table number	Number of patrons	Number of infected	Attack rate (%)	Normalized measured tracer gas concentration	Normalized predicted tracer gas concentration	Normalized predicted exposure to droplet nuclei
TA	10	5	50.00	1.00	1.00	1.00
TB	4	3	75.00	0.87	1.04	0.76
TC	7	2	28.57	0.98	0.93	0.89
T04	0	0	NA	–	1.00	0.00
T05	2	0	0.00	–	0.62	0.07
T06	4	0	0.00	–	0.47	0.13
T07	3	0	0.00	–	0.42	0.04
T08	2	0	0.00	–	0.42	0.06
T09	10	0	0.00	–	0.32	0.04
T10	6	0	0.00	0.55	0.52	0.08
T11	7	0	0.00	–	0.57	0.12
T12	2	0	0.00	–	0.50	0.09
T13	6	0	0.00	–	0.55	0.05
T14	3	0	0.00	–	0.63	0.11
T15	8	0	0.00	0.58	0.54	0.23
T16	5	0	0.00	0.70	0.56	0.06
T17	5	0	0.00	0.86	0.75	0.47
T18	5	0	0.00	0.73	0.85	0.40
Total	89	10	11.24			

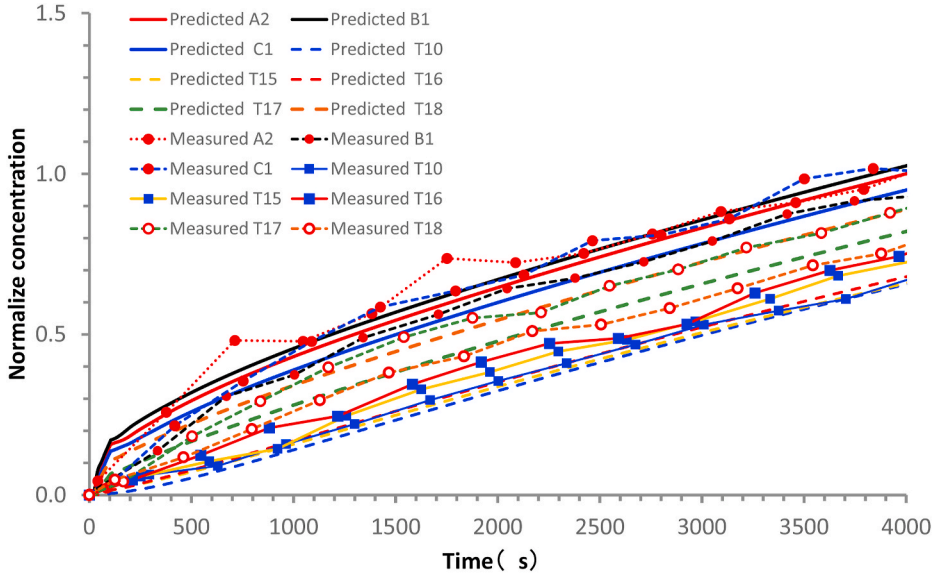

Fig. 5. (Color Online) Comparison between measured and predicted concentrations at monitoring points during exhaled tracer spread test, normalized by the A2 value at 4000 s. (For interpretation of the references to color in this figure legend, the reader is referred to the Web version of this article.)

the additional ABC bubble effect, i.e. the concentrations at other tables become much lower than those at TA–TC (Fig. 7). It should be noted that if the deposition, filtration, and deactivation were not considered, there would also be significant exposure for patrons at Table T17 due to their relative long duration of stay in the restaurant.

The predicted normalized exposure to the exhaled infectious virus droplet nuclei of all tables are also listed in Table 3. According to the results of the logistic regression model, a higher measured concentration of tracer gas is associated with a higher risk of acquiring COVID-19 (odds ratio associated with a 1% increase in concentration: 1.115; 95% CI: 1.009–1.232; $P = 0.033$) (Table 1). Similarly, a higher predicted concentration of tracer gas and higher predicted exposure of the infectious virus-containing droplet nuclei (5 μm) are associated with a higher risk of acquiring COVID-19 (odds ratio associated with a 1% increase in tracer gas concentration: 1.268, 95% CI: 1.029–1.563, $P = 0.026$; odds ratio associated with a 1% increase in exposure of droplet nuclei: 1.079, 95% CI: 1.020–1.142, $P = 0.008$).

4. Discussion

4.1. Poor ventilation and air distribution led to the outbreak

[9] suggested that droplet transmission was the most likely primary cause of this outbreak, but pointed out that the outbreak cannot be explained by droplet transmission alone because the distances between the index case (A1) and patrons at the other tables are all greater than 1 m. We estimate that such distances may have been as great as 4.6 m (Fig. 8). The video records also reveal that the index case never turned their head toward TB during the lunch [9]. also suggested that "strong airflow from the air conditioner could have propagated droplets from table C to table A, then to table B, and then back to table C," but stopped short of pinpointing the role of airborne transmission due to the lack of environmental data. The role of airborne transmission was first postulated by the Chinese National Health Commission (NHC) [16] during the early phase of the COVID-19 epidemic in China; however, no specific evidence is provided in the NHC's recommendation.

Our prediction shows that a contaminated recirculation bubble was

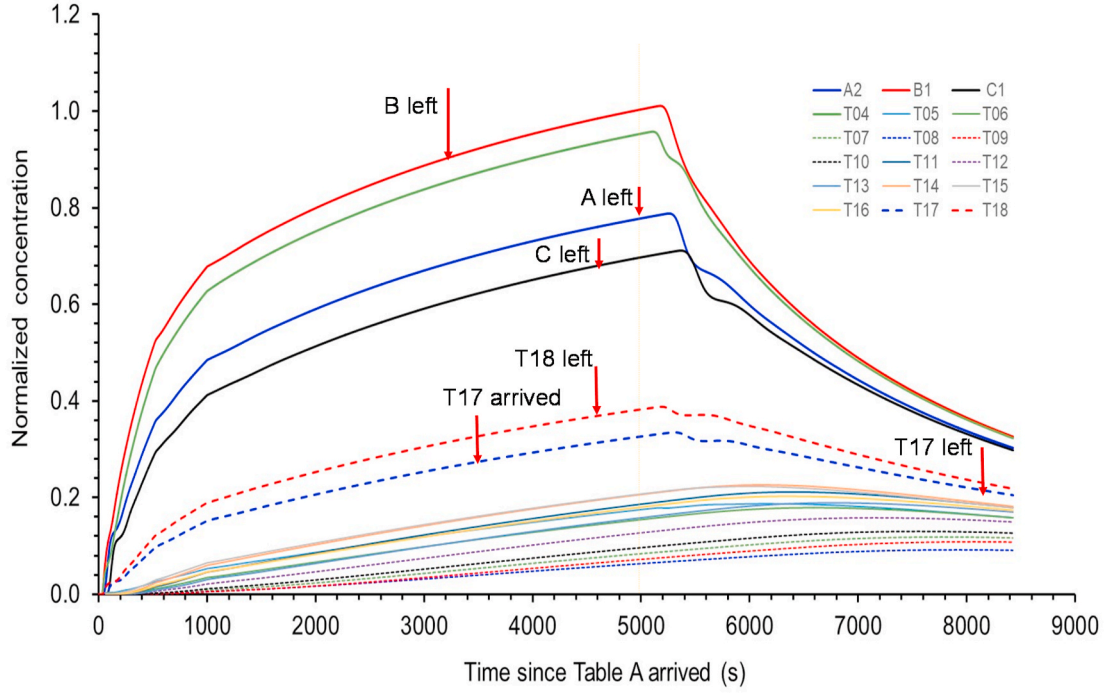

Fig. 6. (Color Online) Predicted concentrations normalized to B1 at 4920 s for some patrons at tables A, B, and C, and other tables after table A patrons arrived at time zero (12:01 p.m.). Table A patrons left the restaurant at time 4920 s (1:22 p.m.). Due to the nature of the air flows, the concentrations for some patrons continued to rise after 4920 s. The results are used to calculate the exposure using the exposure duration data in Table 3. The prediction concentration profiles clearly show a separated ABC zone (i.e., bubble, including T04, which had no patrons), a T17/T18 zone, a zone with T11 and T13–16, and a zone with T07–T10 and T12 close to the outdoor air supply. (For interpretation of the references to color in this figure legend, the reader is referred to the Web version of this article.)

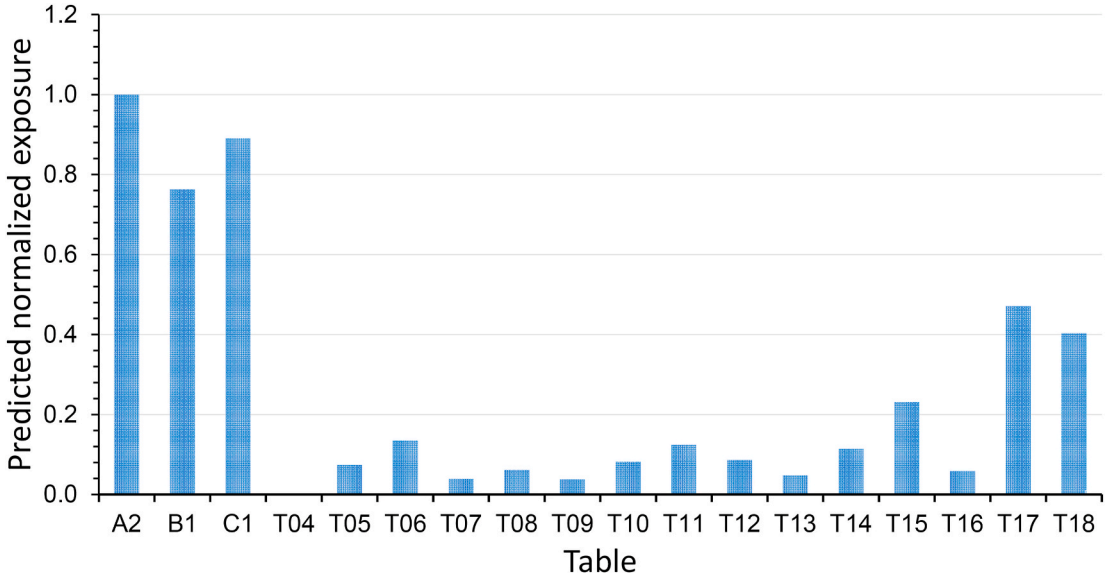

Fig. 7. (Color Online) Predicted exposure of the infectious-virus-containing droplet nuclei normalized to A1 during the entire lunch period at all tables. As no patron was present at Table T04, no exposure can be calculated. (For interpretation of the references to color in this figure legend, the reader is referred to the Web version of this article.)

created in the ABC zone (Fig. 3), which sustained a higher concentration of exhaled droplet nuclei from the index case. The formation of individual circulation zones was due to the spatial configuration of the restaurant and interaction of high-momentum air flow of the five air-conditioning units (Fig. 4). Within the ABC bubble, the infectious virus-containing droplet nuclei would have had time to be deposited, filtered, and deactivated. This is supported by our computer simulation with a measured filtration efficiency of 20% of the 5-μm droplet nuclei, which showed that patrons A2, B1, and C2 were exposed to an average concentration of 0.8, whereas patrons at T17 and T19 were only exposed to an average concentration of 0.3. The overlap period for families A and B in the restaurant was 53 min (between 12:01 and 12:54) and 75 min for families A and C (between 12:03 and 13:18), which would have allowed sufficient exposure time to the exhaled droplets. Patient C1 arrived late, at 12:32, and had a 46-min overlap with family A. That none of the waiters were infected can be attributed to their relatively

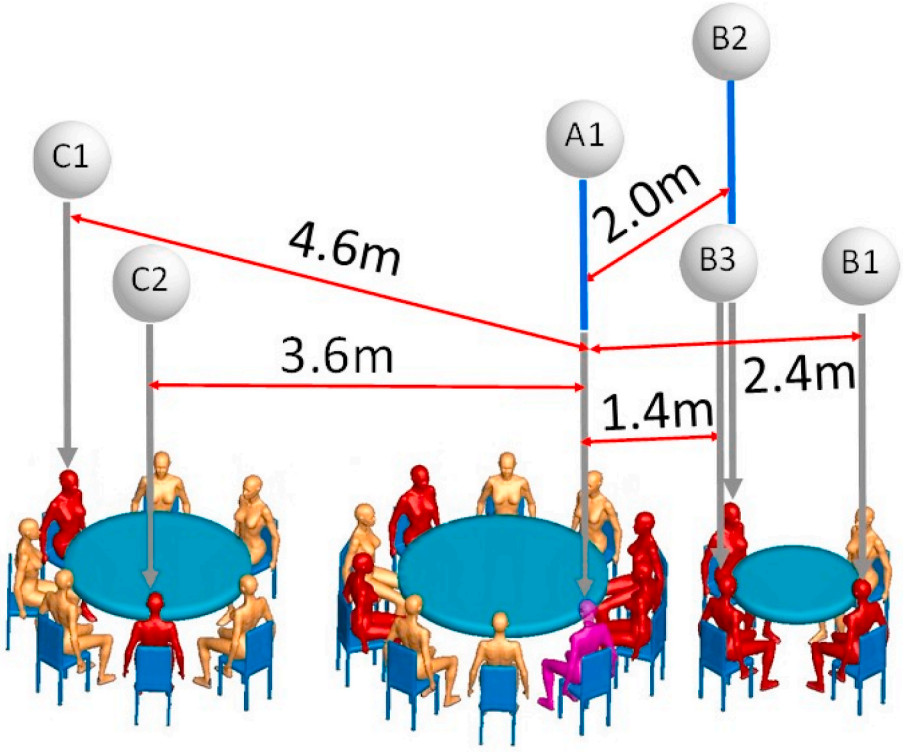

Fig. 8. (Color Online) Distances between index case A1 (purple) and the five infected individuals of families B and C (red). (For interpretation of the references to color in this figure legend, the reader is referred to the Web version of this article.)

short exposure time to exhaled droplets from the index case. A relatively high concentration of tracer gas was also measured at T17 and T18 due to their proximity to the ABC recirculation bubble. Patrons at T17 had only 23 min of overlap with TA but continued to be exposed to the remaining suspended droplet nuclei after family A had left the restaurant. Nevertheless, a low level of exposure to the infectious virus-containing droplet nuclei was predicted because the virus was not only deactivated in aerosols and also removed by deposition and filtration of the air conditioning units as these virus-containing droplet nuclei circulated within the ABC recirculation bubble. None of the patrons at this table ($n = 5$) were infected. Note that additional patrons or restaurant staff may have contracted COVID-19 owing to exposure to the virus in Restaurant X but were asymptomatic, however, asymptomatic infection was paid little attention at the time.

However, the formation of a contaminated recirculation bubble in the ABC zone cannot alone explain the outbreak. Further evidence comes from the low ventilation rates: the observed high concentrations of the simulated contamination result from the lack of outdoor air supply. The exhaust fans in the walls were found to be turned off and sealed during the January 24 lunch, meaning that there was no outdoor air supply aside from infiltration and infrequent and brief opening of the fire door due to the negative pressure generated by the exhaust fan in the restroom. This outdoor air was mainly distributed to the non-ABC zone, thus exacerbating the ventilation deficit of the ABC zone. Ventilation in this study is defined as the supply of outdoor air into the restaurant, and the distribution of the supplied outdoor air in the restaurant. Ventilation is different from air conditioning, however, the supply airflow of the fan coil units, interacting with human body flows, governs the airflow pattern in the restaurant.

The measured averaged ventilation rate of 0.90 L/s per patron in the restaurant is considerably lower than the 8–10 L/s per person required by most authorities or professional societies (e.g., ASHRAE 62.1-2019 [5]). The restaurant was also crowded and extra tables had been added to accommodate the increased number of customers on Chinese New Year's Eve. Consequently, the occupant density was only 1.55 m^2 per patron, including the area occupied by tables. The transmission of SARS-CoV-2, which subsequently resulted in an outbreak of COVID-19, thus occurred in a crowded and poorly ventilated space.

We also attempted to identify the role of fomite and close contact transmission by examining individual trajectories during the patrons' stay in the restaurant from the available video records. We did not find any evidence to support exposure to SARS-Co-V2 via these routes in this instance.

More than two thousands of superspreading events or outbreaks of COVID-19 have been documented by Ref. [17]; who also concluded that "nearly all SSEs [super spreading events] in the database took place indoors." [18] identified 318 outbreaks each with a minimum of 3 cases, comprising a total of 1245 confirmed cases in 120 prefectural cities in non-Hubei provinces, China, and found that none occurred in outdoor settings. High attack rates of COVID-19 have also been found in choir rehearsal [8,19], homeless shelters [20–22]; nightclubs [23]; Fitness centers [24,25] and meat processing plants [26]. Although airborne transmission has been suspected in many of these outbreaks, ventilation rates were not measured in the infection venues.

4.2. Estimation of quanta generation

Estimation of quanta generation in this outbreak is challenging as the flow is not fully mixed. However, it might still be useful to offer an estimation based on the fully mixing condition. The volume of air in the restaurant is 431 m^3. The averaged air change rate during two measurements were 0.67 h^{-1}. We adopted an aerosol deposition rate of 0.3 h^{-1} and virus deactivation rate of 0.63 h^{-1} [8]. The pulmonary flow rate for restaurant setting is 1.65 m^3/h. As the effective air change rate is only 1.60 h^{-1}, the transient Wells-Riley equation needs to be used, which gives an estimated quanta generation rate of 79.3 quanta/h, which is compared with 970 ± 390 quanta/h in a choir rehearsal outbreak [8], about 5.0 quanta/h in light exercise with speaking conditions by Buonanno et al. [6], and 14–48 quanta/h using a reproductive number-based fitting approach [7]. According to Ref [27], "…

infectiousness profile of a typical SARS-CoV-2 patient peaks just before symptom presentation", which is also supported by other studies (e.g. Refs. [28–30]. Our estimated relatively large quanta generation rate for the pre-symptomatic index case is also in agreement with this theory of peak infectiousness just before the symptom presentation, as the index case only developed symptoms after the lunch, and she seemed having not infected others elsewhere.

To ensure that there is less than one person to be infected in the restaurant, the estimated minimum ventilation rate becomes 38.6 L/s per person using the estimated quanta value. This estimated minimum ventilation rate is much larger than the required minimum ventilation rate of 5.1 L/s per person in restaurants/dining rooms by international ventilation standards such as ASHRAE 62.1-2019 [5].

4.3. Importance of sufficiently low occupancy and other intervention

Lack of adequate ventilation and overcrowding is known to be associated with respiratory infection outbreaks, although some are not commonly thought to be transmitted by aerosols. This restaurant SARS-CoV-2 outbreak resembles the Alaska plane influenza outbreak [31], in which a plane with a 56-seat passenger compartment was delayed by engine trouble and no mechanical ventilation was provided during the 4.5-h wait. The index case was a passenger who became ill with influenza within 15 min after boarding the plane. There was approximately 3 m^3 of compartment space per seat, and the provision of outdoor air was only possible by the plane doors being open for some periods during the 4.5-h wait and during the movement of passengers in and out of the plane. According to Ref. [32]; this resulted in there being only 0.08–0.40 L/s of air circulation per passenger, which is slightly less than the range measured in Restaurant X, and this resulted in 72% of the 54 passengers on board this plane being infected with influenza.

A systematic review by the World Health Organization (WHO) also found evidence for the association between crowding and infection [33]. During the 2009H1N1 pandemic, the basic reproduction number was as high as 3.0–3.6 in outbreaks in crowded schools, compared to 1.3–1.7 in less crowded settings [34,35]; Writing Committee, 2010). The SARS-CoV-2 virus can survive in air for at least 3 h [15] and airborne influenza virus genomes and viable influenza virus particles have been detected [36–39].

It is important to note that our results do not indicate that long-range airborne transmission of SARS-CoV-2 can occur in any indoor space, but rather that transmission may occur in a crowded and poorly ventilated space. Gao et al. [40] showed that the relative contribution of aerosols to respiratory infection is a function of ventilation flow rate. A sufficiently high ventilation flow-rate reduces the contribution of airborne transmission to a very low level, whereas a low ventilation flow-rate leads to a relatively high contribution of aerosols to transmission. For airborne transmission of respiratory infection such as COVID-19, the infectious virus is carried by aerosols. These aerosols can be not only removed by ventilation, but also by deposition and filtration, and the virus in aerosols can be deactivated, e.g. by ultraviolet germicidal irradiation (UVGI). Therefore, in addition to ventilation, effectiveness of other aerosol removal, and/or virus deactivation methods should be explored.

In summary, our epidemiologic analysis, onsite experimental tracer measurements, and airflow simulations support the probability of a long-range aerosol spread of the SARS-CoV-2 having occurred in the poorly ventilated and crowded Restaurant X on January 24, 2020.

This conclusion has important implications for intervention methods in the ongoing COVID-19 pandemic. Our study suggests that it is crucial to prevent overcrowding and provide good ventilation and effective air distribution in buildings and transport cabins to prevent the spread of SARS-CoV-2 and the development of COVID-19.

Author contributions

Y. Li, H. Qian, J. Hang and M. Kang contributed equally. Y. Li, M. Kang, and H. Qian contributed to the study design, hypothesis formulation, and coordination. H. Qian led the CFD modeling. J. Hang led the field environmental experiments. M. Kang, J. Li, and X. Chen, contributed to the field investigation, data analyses, and reporting. X. Chen, P. Liang, and H. Ling contributed to the field studies and experiments. J. Wei and L. Liu contributed to experimental design. S. Wang contributed to CFD modeling. S. Xiao contributed to the statistical analysis. Y. Li wrote the first draft of the paper. M. Kang, H. Qian, J. Hang, and X. Chen contributed to major manuscript revisions. All of the other authors contributed to revisions.

Funding

This work was supported by the Research Grants Council of Hong Kong's General Research Fund [grant number 17202719]; Research Grants Council of Hong Kong's Collaborative Research Fund [grant number C7025-16G]; the National Key Research and Development Program of China [grant number 2017YFC0702800]; the National Natural Science Foundation of China [grant number 41875015]; and the Science and Technology Planning Project of Guangdong Province [grant number 2019B111103001].

The authors are grateful to colleagues at Guangzhou CDC, Guangzhou Yuexiu CDC, and Guangdong CDC who helped in collecting the epidemiologic data, and to Professor Bao Ruoyu and students of Sun Yat-sen University for assisting with the field experiments.

Declaration of competing interest

The authors declare that they have no known competing financial interests or personal relationships that could have appeared to influence the work reported in this paper.

Appendix E. Supplementary data

Supplementary data related to this article can be found at https://doi.org/10.1016/j.buildenv.2021.107788.

Appendix A. Basic patient information

Table A.1
Basic patient information.

Case	Family data	Basic data	Symptom onset date	Symptoms	Confirmation date
A1	Residents of Wuhan, arrived in Guangzhou on Jan. 22. Family A includes four small families: the family of the index case including their husband and grandson ($n = 3$); mother-in-law's family ($n = 2$); sister's family ($n = 2$); and niece's family ($n = 3$)	female, 63 y.o., history of hypertension, hyperlipidemia, and cervical spondylosis.	Jan. 24	Fever (37.5 °C), dry cough	Jan. 26
A2			Jan. 27	Fever (37.8 °C)	Jan. 27

(*continued on next page*)

Table A.1 (*continued*)

Case	Family data	Basic data	Symptom onset date	Symptoms	Confirmation date
		female, 60 y.o., younger sister of case A1, was in good health.			
A3		female, 62 y.o., mother-in-law of A1's son, was in good health.	Jan. 29	Fever (37.3 °C)	Jan. 30
A4		female, 34 y.o., niece of A1, was in good health.	Jan. 29	Fever (not recorded)	Jan. 30
A5		male, 63 y.o., father-in-law of A1's son, was in good health.	Feb. 2	Fever (not recorded)	Feb. 3
B1	Residents of Guangzhou. Family B ($n = 4$) includes one family, although the older mother lived alone.	female, 44 y.o., was in good health.	Feb. 1	Fever (38.4 °C), cough, sputum	Feb. 4
B2		female, 20 y.o., daughter of B1, was in good health.	Feb. 3	diarrhea and fever (38.6 °C), dry cough, chest tightness, asthma	Feb. 6
B3		male, 53 y.o., husband of B1, was in good health.	Feb. 5	headache, chest tightness, chest pain, bloating	Feb. 6
C1	Residents of Guangzhou. Family C includes three small families: the patient couple and mother ($n = 3$); their son's family ($n = 2$); and brother's family ($n = 2$).	female, 82 y.o., retired, was in good health.	Jan. 27	Fever (37.8 °C), runny nose, cough, sputum	Feb. 10
C2		female, 54 y.o., daughter of C1, was in good health.	Jan. 31	fever (39.9 °C), dry cough	Feb. 6

Appendix B. Airflow and dispersion video

Movie B.1 Spread of exhaled droplet nuclei in the restaurant as predicted by computational fluid dynamics. Red indicates the highest concentrations and blue the lowest. (see file: Movie mp4- Spread of exhaled tracer gas in Restaurant X.mp4).

Supplementary video related to this article can be found at https://doi.org/10.1016/j.buildenv.2021.107788

Appendix C. Some measurement details

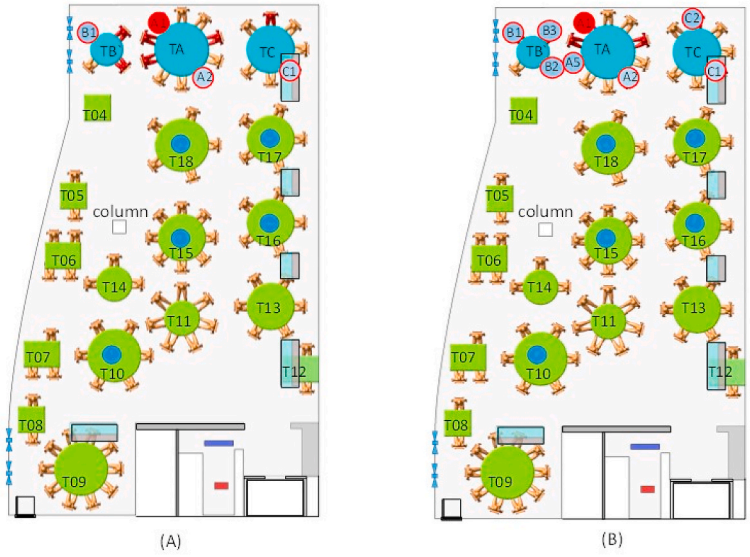

Fig. C.1. (Color Online) Location of tracer gas (ethane) concentration sensors on the floor plan during the (A) afternoon test and (B) morning test with a leak. The red seat indicates the position of index case A1. Small red-outlined circles indicate the seating location of the infected patrons. Small blue circles indicate the location of the tracer gas sensors. The tables are numbered TA, TB, and TC for families A, B, and C, respectively, and T04–T18 for the other tables. The morning test with a leak was unintended; the tracer gas leaked due to a damaged pipe below TA. Nevertheless, the measured data from test (B) also support the observed distribution in test (A).

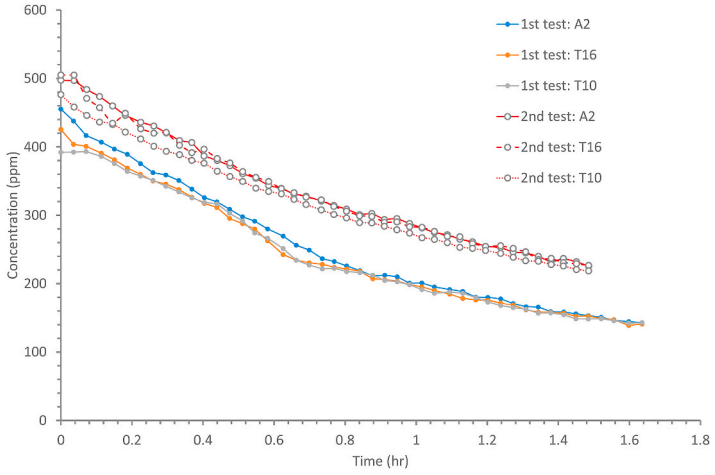

Fig. C.2. (Color Online) Measured tracer gas concentration profile from the two tracer gas decay tests for ventilation rate measurement. The concentrations were monitored at three locations during each test: seat A2, Table 10 (T10), and Table 16 (T16). For each test, the three curves are reasonably close, suggesting the room air flow was reasonably fully mixed by using the mixing fans during the test.

Appendix D. Guangzhou epidemiological data

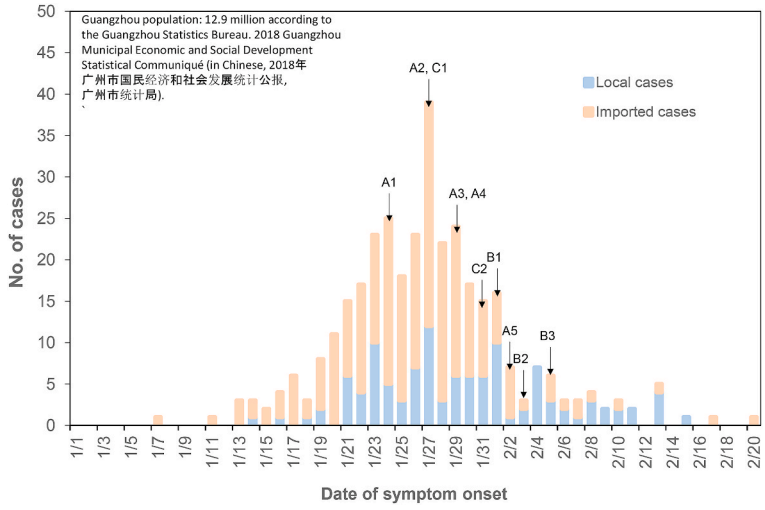

Fig. D.1. (Color Online) The epidemiological curve in Guangzhou (population 12.9 million), where restaurant X is located and where families B and C live. The symptom onset dates of all infected members of families A, B, and C are also shown. By January 24, when A1 had the first symptoms, there were 72 symptomatic cases (15 local and 59 imported); by January 27, when C1 had the first symptoms, there were 202 symptomatic cases (52 local and 150 imported); and by Feb 1, when B1 had the first symptoms, there were 296 symptomatic cases (83 local and 213 imported). With close contact tracing, families B and C did not have contact with any of the identified cases and/or any visitors from Hubei Province 14 days prior to the onset of their symptoms.

References

[1] L. Morawska, J. Cao, Airborne transmission of SARS-CoV-2: the world should face the reality, Environ. Int. 139 (2020) 105730.
[2] USA Centers for Disease Control and Prevention CDC, How 2019-nCoV Spreads, U. S. Department of Health & Human Services, Washington DC, USA, 2020. https://www.cdc.gov/coronavirus/2019-ncov/about/transmission.html.
[3] World Health Organization, Coronavirus disease (COVID-19): how is it transmitted?. https://www.who.int/news-room/q-a-detail/coronavirus-disease-covid-19-how-is-it-transmitted. (Accessed 9 July 2020) (Accessed on 15 November 2020).
[4] E.C. Riley, G. Murphy, R.L. Riley, Airborne spread of measles in a suburban elementary school, Am. J. Epidemiol. 107 (5) (1978) 421–432.
[5] American Society of Heating, Refrigerating and Air-Conditioning Engineers (ASHRAE) Ventilation for Acceptable Indoor Air Quality, vol. 62, ASHRAE Standard, Atlanta, USA, 2019, 1.
[6] G. Buonanno, L. Stabile, L. Morawska, Estimation of airborne viral emission: quanta emission rate of SARS-CoV-2 for infection risk assessment, Environ. Int. 141 (2020) 105794.
[7] H. Dai, B. Zhao, Association of the infection probability of COVID-19 with ventilation rates in confined spaces, Building Simulation 13 (2020) 1321–1327, 1-7.
[8] S.L. Miller, W.W. Nazaroff, J.L. Jimenez, et al., Transmission of SARS-CoV-2 by inhalation of respiratory aerosol in the Skagit Valley Chorale superspreading event, Indoor Air (2021) 3141–32310, 0; 0031.
[9] J. Lu, J. Gu, K. Li, et al., COVID-19 outbreak associated with air conditioning in restaurant, Guangzhou, China, Emerg. Infect. Dis. 26 (7) (2020) 1628.
[10] Y. Li, X. Huang, I.T.S. Yu, et al., Role of air distribution in SARS transmission during the largest nosocomial outbreak in Hong Kong, Indoor Air 15 (2005) 83–95.
[11] T.W. Wong, C.K. Li, W. Tam, et al., Cluster of SARS among medical students exposed to single patient, Hong Kong, Emerg. Infect. Dis. 10 (2004) 269–276.
[12] I.T.S. Yu, Y. Li, T.W. Wong, et al., Evidence of airborne transmission of the severe acute respiratory syndrome virus, N. Engl. J. Med. 350 (2004) 1731–1739.
[13] M. Bivolarova, J. Ondráček, A. Melikov, et al., Comparison between tracer gas and aerosol particles distribution indoors: the impact of ventilation rate, interaction of airflows, and presence of objects, Indoor Air 27 (6) (2017) 1201–1212.
[14] S. Holmberg, Y. Li, Modelling of indoor environment - particle dispersion and deposition, Indoor Air 8 (2) (1998) 113–122.

[15] N. van Doremalen, D.H. Morris, M.G. Holbrook, et al., Aerosol and surface stability of SARS-CoV-2 as compared with SARS-CoV-1, N. Engl. J. Med. 382 (16) (2020) 1564–1567.
[16] X. Li, F. Gao, Public prevention guidelines of infection due to the novel coronavirus pneumonia, in: Chinese, 新型冠状病毒感染的肺炎公众防护指南, vol. 9, People's Medical Publishing House, Beijing, China, 2020.
[17] K. Swinkels, SARS-CoV-2 Superspreading events around the world, Accessed on 29 December 2020, https://kmswinkels.medium.com/covid-19-superspreading-events-database-4c0a7aa2342b, 2020.
[18] H. Qian, T. Miao, L. Liu, et al., Indoor transmission of SARS-CoV-2, Indoor Air (2020), https://doi.org/10.1111/ina.12766.
[19] N. Charlotte, High rate of SARS-CoV-2 transmission due to choir practice in France at the beginning of the COVID-19 pandemic, J. Voice (2020), https://doi.org/10.1016/j.jvoice.2020.11.029.
[20] E. Imbert, P.M. Kinley, A. Scarborough, et al., Coronavirus Disease 2019 (COVID-19) Outbreak in a San Francisco Homeless Shelter, Clinical Infectious Diseases, 2020, p. ciaa107.
[21] M. Ralli, A. Morrone, A. Arcangeli, et al., Asymptomatic patients as a source of transmission of COVID-19 in homeless shelters, Int. J. Infect. Dis. 103 (2021) 243–245, 0.
[22] F.A. Tobolowsky, E. Gonzales, J.L. Self, et al., COVID-19 outbreak among three affiliated homeless service sites-King County, Washington, 2020, MMWR (Morb. Mortal. Wkly. Rep.) 69 (17) (2020) 523. Updated on 28 October 2020. (Accessed 15 November 2020).
[23] C.R. Kang, J.Y. Lee, Y. Park, et al., Coronavirus disease exposure and spread from nightclubs, South Korea, Emerg. Infect. Dis. 26 (10) (2020) 2499.
[24] S. Bae, H. Kim, T.Y. Jung, et al., Epidemiological characteristics of COVID-19 outbreak outbreak at fitness fitness centers centers in cheonan, korea, J. Kor. Med. Sci. 35 (31) (2020) e288.
[25] S. Jang, S.H. Han, J.Y. Rhee, Cluster of coronavirus disease associated with fitness dance classes, South Korea, Emerg. Infect. Dis. 26 (8) (2020) 1917.
[26] T. Günther, M. Czech-Sioli, D. Indenbirken, et al., SARS-CoV-2 outbreak investigation in a German meat processing plant, EMBO Mol. Med. 12 (2020), e13296.
[27] K. Sun, W. Wang, L. Gao, et al., Transmission heterogeneities, kinetics, and controllability of SARS-CoV-2, Science 371 (2021) 254–2540.
[28] M. Cevik, M. Tate, O. Lloyd, et al., SARS-CoV-2, SARS-CoV, and MERS-CoV viral load dynamics, duration of viral shedding, and infectiousness: a systematic review and meta-analysis, The Lancet Microbe 2 (1) (2021) e13–e22, 0.
[29] X. He, E.H. Lau, P. Wu, et al., Temporal dynamics in viral shedding and transmissibility of COVID-19, Nat. Med. 26 (5) (2020) 672–675.
[30] W.E. Wei, Z. Li, C.J. Chiew, et al., Presymptomatic transmission of SARS-CoV-2-Singapore, january 23-march 16, 2020, MMWR (Morb. Mortal. Wkly. Rep.) 69 (14) (2020) 411.
[31] M.R. Moser, T.R. Bender, H.S. Margolis, et al., An outbreak of influenza aboard a commercial airliner, Am. J. Epidemiol. 110 (1) (1979) 1–6.
[32] S.N. Rudnick, D.K. Milton, Risk of indoor airborne infection transmission estimated from carbon dioxide concentration, Indoor Air 13 (3) (2003) 237–245.
[33] World Health Organization, WHO housing and health guidelines. https://www.who.int/sustainable-development/publications/housing-health-guidelines/en/. (Accessed 23 November 2018) (Accessed on 15 November 2020).
[34] J. Lessler, N.G. Reich, D.A. Cummings, et al., Outbreak of 2009 pandemic influenza A (H1N1) at a New York City school, N. Engl. J. Med. 361 (27) (2009) 2628–2636.
[35] Writing Committee of the WHO Consultation on Clinical Aspects of Pandemic H1N1, Influenza. Clinical aspects of pandemic 2009 influenza A (H1N1) virus infection, N. Engl. J. Med. 362 (18) (2009) 1708–1719, 2010.
[36] W.G. Lindsley, T.A. Pearce, J.B. Hudnall, et al., Quantity and size distribution of cough-generated aerosol particles produced by influenza patients during and after illness, J. Occup. Environ. Hyg. 9 (7) (2012) 443–449.
[37] W.G. Lindsley, F.M. Blachere, D.H. Beezhold, et al., Viable influenza A virus in airborne particles expelled during coughs versus exhalations, Influenza and other respiratory viruses 10 (2016) 404–413.
[38] C. Xie, E.H. Lau, T. Yoshida, et al., Detection of influenza and other respiratory viruses in air sampled from a university campus: a longitudinal study, Clin. Infect. Dis. 70 (5) (2020) 850–858.
[39] J. Yan, M. Grantham, J. Pantelic, et al., Infectious virus in exhaled breath of symptomatic seasonal influenza cases from a college community, Proc. Natl. Acad. Sci. Unit. States Am. 115 (2018) 1081–1086.
[40] X. Gao, J. Wei, P. Xu, et al., Building ventilation as an effective disease intervention strategy on a large and dense social contact network, PLos One 11 (9) (2016) e0162481, https://doi.org/10.1371/journal.pone.0162481.